A new time-of-flight technique: experiments conducted on oxygen-rich PDATS crystals

1993 J. Phys.: Condens. Matter 5 85

(http://iopscience.iop.org/0953-8984/5/1/009)

J. Phys.: Condens. Matter 5 (1993) 85–94. Printed in the UK

A new time-of-flight technique: experiments conducted on oxygen-rich PDATS crystals

N E Fisher
Department of Physics, King's College London, Strand WC2R 2LS, UK

Received 21 September 1992

Abstract. A novel time-of-flight technique for determining carrier transport in a photoconductive crystal is desribed. Parallel wires with a small spacing are laid down above but not touching the crystal and are positioned perpendicular to carrier drift. A photo-generated carrier sheet (of one sign) drifting under the wires induces currents on those wires and it is the inspection of these current profiles that gives information about carrier drift velocity, mobility and, in addition, a qualitative observation of the the time evolution of the spread of the carrier sheet with field and distance traversed. These experiments are conducted on oxygen-rich polydiacetylene PDATS crystals (but could in principle be used on other materials) and the conclusions reached using this technique are found to agree with those obtained using another time-of-flight technique also briefly described.

1. Introduction

The aim of this paper is to present some results using a new (as far as the author is aware) time-of-flight experimental technique for deducing the charge transport properties of a photo-generated carrier sheet under the action of an applied field. These experiments are conducted on the polymer bis(*p*-toluene sulphonate) ester of 2,4-hexadiyne-1,6-diol (PDATS) but in principle could be used on other materials. Before describing the action of this technique we shall briefly review the background of PDATS and in particular its charge transport properties as deduced using a more conventional time-of-flight technique. These latter results are then used as a comparison for the experiments presented here.

PDATS is easily produced as millimetre-sized single crystals in which the polymer backbone direction is well defined and common to all chains in the sample [1]. Because the chain separation is large (0.7 nm) compared with the repeat unit distance on a chain (0.45 nm) [2], each chain may be considered as an independent quasi-one-dimensional semiconductor. Dark conductivity measurements along and perpendicular to the chains made by Siddiqui and Wilson [3] show an anisotropy of over 1000 reflecting this one-dimensional nature. The interest in PDATS, then, is that it offers an insight into quasi-one-dimensional carrier motion.

There is, however, some controversy concerning the drift of these photo-generated carriers along the polymer chains: Donovan and Wilson (DW) [4, 5] interpret their photoconductivity experiments (which are not time-of-flight) as demonstrating carrier drift that is electric field saturated at a velocity that is comparable to the speed of sound along the chain direction (about 5000 m^{-1} [6]), down to the smallest fields (10^2

0953-8984/93/010085+10$07.50

$V\ m^{-1}$) at which their measurements prove possible. An ultra-high low-field mobility in excess of 20 $m^2\ s^{-1}\ V^{-1}$ is deduced. In addition, they also claim an inter-trap separation of the order of 1 mm [7]. Thus, DW conclude that they are observing the intrinsic trap-free drift of the carriers for macroscopic distances along the polymer chains. On the other hand (using similar experimental techniques), Heeger *et al* [8, 9] report a carrier drift velocity that is linearly proportional to the applied field, while Blum and Bassler [10] deduce a carrier drift that is weakly field dependent at low field ($< 0.5\times10^6\ V\ m^{-1}$) and increases linearly proportionally to the applied field at higher field. These latter two groups also report carrier drift that is acoustic and trap-limited with inter-trap separations microns apart, and observed trap-limited mobilities of the order of $10^{-4}\ m^2\ s^{-1}\ V^{-1}$.

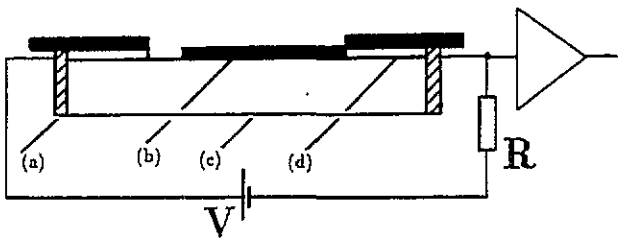

Figure 1. Arrangement (side view) of surface configuration transit current experiments: (a) silver-paste, (b) optical mask with slit, (c) PDATS crystal, (d) evaporated Ag electrode. Following a laser pulse, carriers are generated at the slit. Depending on the polarity of V, one sign of carrier traverses the sample to induce a transit signal, while the other sign discharges almost immediately at its nearest electrode.

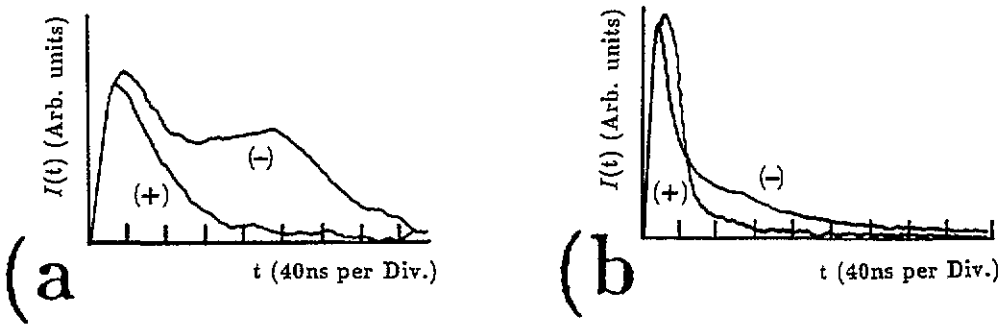

Figure 2. Transit currents obtained using: (a) an oxygen-free sample of length 240 μm with an applied field of $2.9\times10^6\ V\ m^{-1}$ and (b) an oxygen-rich sample of length 240 μm with an applied field of $8.3\times10^6\ V\ m^{-1}$. (-) left electrode negative, (+) left electrode positive.

Recently Fisher and Willock [11], using a surface configuration of the classic Kepler/LeBlanc [12, 13] time-of-flight experimental arrangement (figure 1), find trap-limited time-of-flight signals for electrons only and corresponding featureless decays for the holes (as in figure 2), down to sample lengths of 50 μm. We concluded therefore that the electrons were the dominant current carriers. Furthermore, the

drift velocities of the electrons were found to be acoustic (varying from 400 m s^{-1} to about 3000 m s^{-1} for applied electric fields of 0.5×10^6 V m^{-1} to about 7.0×10^6 V m^{-1}) with observed trap-limited mobilities of the order of 10^{-4} m^2 s^{-1} V^{-1}. In addition, the time-of-flight profiles were found to become more ill-defined (tending towards featureless decays) as the applied fields were reduced ($<0.5\times10^6$ V m^{-1}), and this we attributed to increased dispersive carrier propagation due to a lengthening of field-dependent trap-release times.

Thus, broadly speaking, our results were in agreement with those of Heeger and Bassler but not, in our opinion, reconcilable with those of DW.

We also found that those crystals grown in an oxygen-free environment (to be termed oxygen-free crystals) exhibited significantly less deep and shallow trap concentrations than those grown in the presence of oxygen (oxygen-rich crystals) [14]. This can be clearly seen from figure 2 which shows a comparison of the transit signals obtained using these two types of crystal. Only at the highest fields (well in excess of 5.0×10^6 V m^{-1}) do the oxygen-rich crystals exhibit a time-of-flight profile and even this is almost featureless. This to us was strongly suggestive of dispersive (non-Gaussian) transient transport (Pfister and Scher [15], Scher and Montroll [16]), a conclusion also reached by Siddiqui [17] in his attempts to find time-of-flight signals.

Finally, amongst a series of novel experiments, Yang *et al* [18] claim (using time-of-flight techniques) to have observed field saturation of carriers in the field range 0.8 to 1.5×10^6 V m^{-1}, with drift velocities one order of magnitude higher ($5–6\times10^4$ m s^{-1}) than those previously reported. We suggested in our transit current paper [11], however, that because their laser intensities and hence carrier densities were considerably higher than our own, and also because none of their photo-currents exhibited a plateau or tail (a profile usually associated with time-of-flight signals), those experiments may have been conducted under severe space charge conditions in which the photo-generated carrier sheets appreciably disturb the applied electric field [19, 20, 21] and so, in our opinion, led to some doubt as to the validity of the interpretations of their photo-currents.

We now describe a novel time-of-flight technique. These experiments are performed on oxygen-rich crystals with the aim of deducing carrier drift velocities and carrier mobilities—something that was difficult to achieve using the more conventional time-of-flight methods.

2. Experimental method and operation

The experimental arrangements are shown in figures 3: parallel wires with a small spacing d, evaporated onto transparent Mylar, are laid down above but not touching the crystal's (100) face and are positioned so that they are perpendicular to the polymer chains. Sandwiched between the wires and the face is an opaque dielectric optical mask with a slit. This slit is positioned (again perpendicular to the polymer chains) between two of the wires. Following a fast laser pulse incident on the mask coupled with an applied electric field ($F = 2V/D$) across the crystal (and parallel to the polymer chains), electron–hole pairs are generated in the region of the slit. Hence, under the action of the applied field, two carrier sheets of opposite sign, initially generated there, will drift in opposite directions under the wires inducing (as they drift) currents on those wires. As will become clear, it is the inspection of these

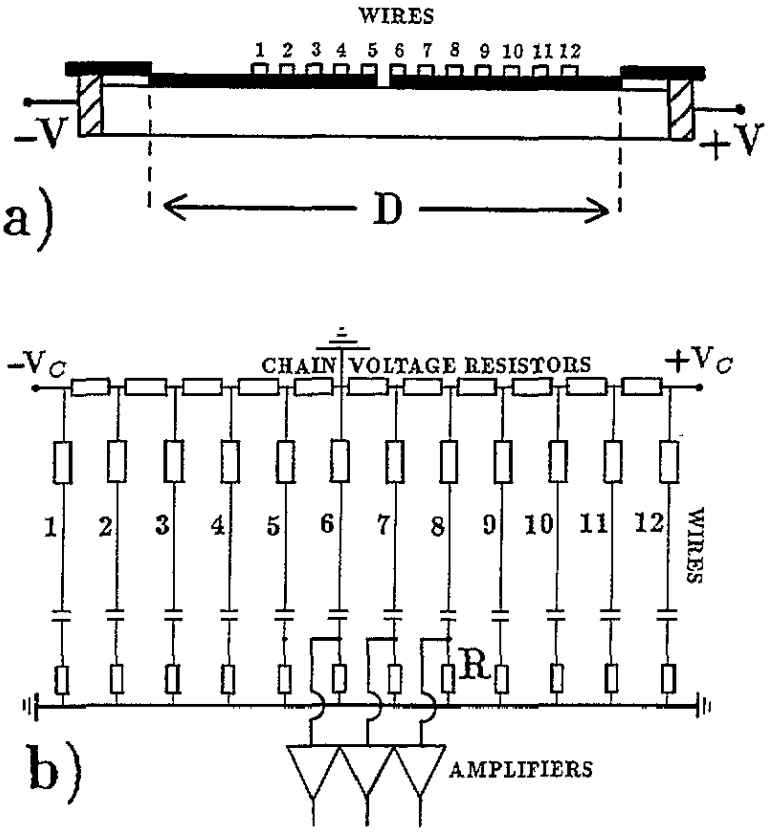

Figure 3. Experimental set-up for wires experiment. (a) shows the side view of the wires/mask/sample arrangement and (b) shows the top view of the wires. The wires are positioned perpendicular to the direction of carrier drift. By suitable application of $\pm V_c$, potentials are generated across each of the wires which correspond to those on the sample face under them.

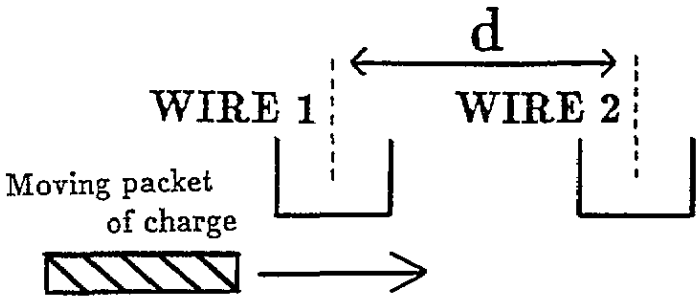

Figure 4. Carrier sheet drifting under two wires (1 and 2).

induced current profiles that will yield information about the transport properties of these carrier sheets.

Figure 4 shows a carrier sheet drifting at constant velocity towards, under, and

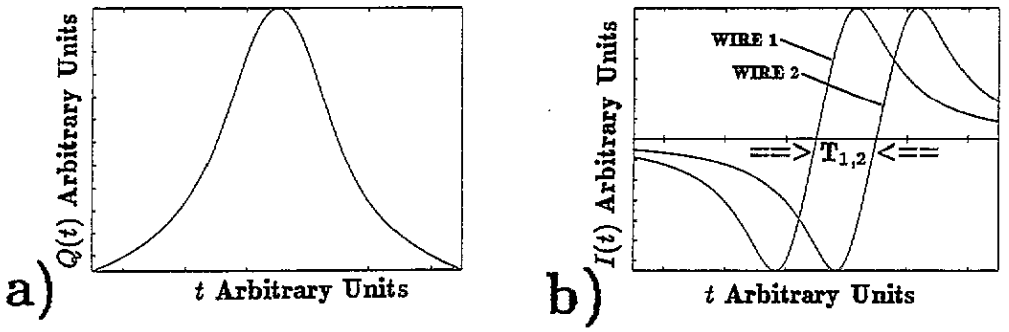

Figure 5. Induced charge on wire 1 and induced currents on adjacent wires 1 and 2, expected to resemble those shown in (a) and (b) respectively.

away from, two adjacent wires (1 and 2) of spacing d, under ideal experimental conditions (that is, with no diffusion or dispersion present). We would expect, then, the induced charge $Q(t)$ on one of the wires to resemble that in figure 5(a) where its maximum value corresponds to the centre of charge of the carrier sheet drifting directly under one of the wires. However, from the arrangement of figure 3(b), what will actually be observed in experiment is the induced current which is given by

$$I(t) = -\mathrm{d}Q(t)/\mathrm{d}t. \tag{1}$$

This we show in figure 5(b) for the two wires. (Here we have assumed that interactions between adjacent wires are small compared to that induced by the moving charge.) It is obvious that in this simple scenario the current reversals are of equal magnitude because there is no diffusion or dispersion present (i.e. the carrier sheet remains as a sheet as it drifts) and that the point at which the currents reverse sign (henceforth referred to as the crossover points) corresponds to the position at which the sheet's centre of charge is directly under the induced current's respective wire. Thus, ideally, it should be possible to track the centre of charge of the carrier sheet as it traverses the crystal with, in this case, its velocity between wires 1 and 2 given by

$$v_\mathrm{d} = d/T_{1,2} \tag{2}$$

and hence its mobility given by

$$\mu = v_\mathrm{d}/F. \tag{3}$$

For the experiments presented here then, the wires, each of width 10–15 μm, are about 30 μm above the sample surface with their spacing d equal to 50 μm. D (the inter-electrode distance) is 1 mm. The laser pulse used is of intensity about 10^7 W m^{-2}, photon energy 3.68 eV and duration 10 ns (FWHM), and generates carriers in a skin depth of about 0.5 μm. The induced currents are recorded using a fast oscilloscope (Tektronix 7A26) and amplifier system (LM733 video differential

amplifiers) having an overall response time of about 10 ns. All experiments are conducted under a vacuum of 10^{-6} Torr.

We finally note an important point from figure 3(b): during the experiment, potentials are applied across each of the wires via the chain voltage resistors shown, which act as a potential divider. Their purpose, by applying suitable values of $-V_c$ and $+V_c$ across the divider, is to minimize the effect that the wires have in disturbing the applied field across the crystal by generating an equivalent field across the wires. Thus, from the arrangement of figure 3(a) (which is in a sense arbitrary), wire 6, which is earthed, will be centred midway between the surface electrodes.

3. Results and discussion

Figures 6(a) and 6(b) show the currents induced on wires 6, 7 and 8 and those induced on wires 8, 9 and 10 respectively, by negative carriers drifting under them. By simply reversing the polarity of the applied field (and V_c), the corresponding currents induced by the holes may be observed and are shown in figures 7(a) and 7(b). It is immediately apparent from comparison of these two sets of profiles that the electrons are the dominant current carriers since no obvious current reversal is observed for the hole signals. However, it is probably not correct to conclude from this that these holes are stationary (as opposed to slowly drifting) and that what is actually being seen is the drift of electrons in the opposite direction, since it is possible that a very small hole current reversal may occur but at long times. Unfortunatly, such a reversal, if it exists, is difficult to detect using the fast amplifiers employed here.

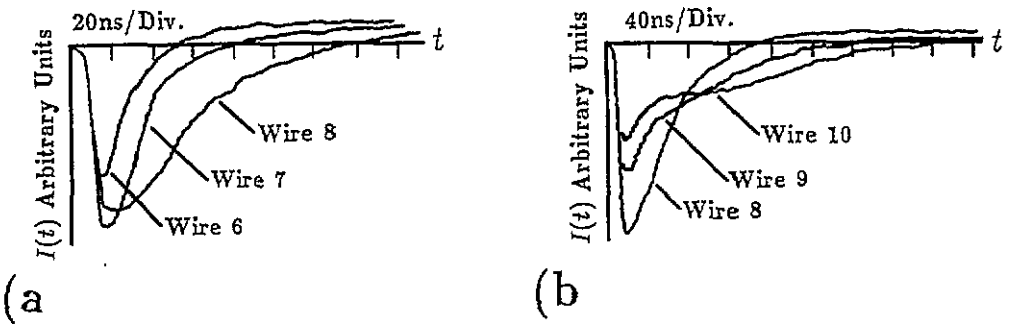

Figure 6. Currents on (a) wires 6, 7, and 8 and (b) wires 8, 9, and 10 induced by electrons drifting in an applied field of 3.4×10^6 V m^{-1}.

Figure 8 shows the field dependence of the current profiles induced by the electrons on the first three wires, and in particular their crossover points.

From all these data, we see that the profiles are more complex than the simple model of section 2: there is an initial photo-peak, which is a convolution of carrier generation and subsequent drift and which essentially follows the light pulse, and superimposed on that (at least for the electron case) is the drift of carriers under the wires. In addition, these profiles are also highly asymmetric, indicating considerable dispersion of the carrier sheet at early times. We see that by reducing the applied field,

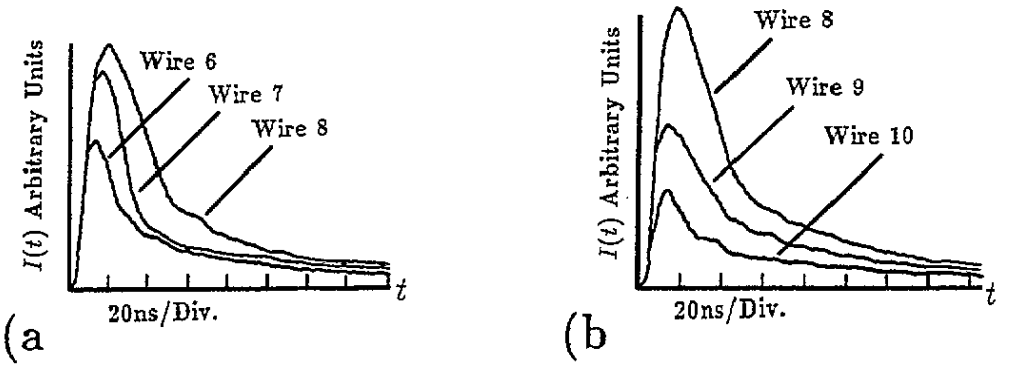

Figure 7. Currents on (a) wires 6, 7, and 8 and (b) wires 8, 9, and 10 induced by holes drifting in an applied field of 3.4×10^{6} V m^{-1}.

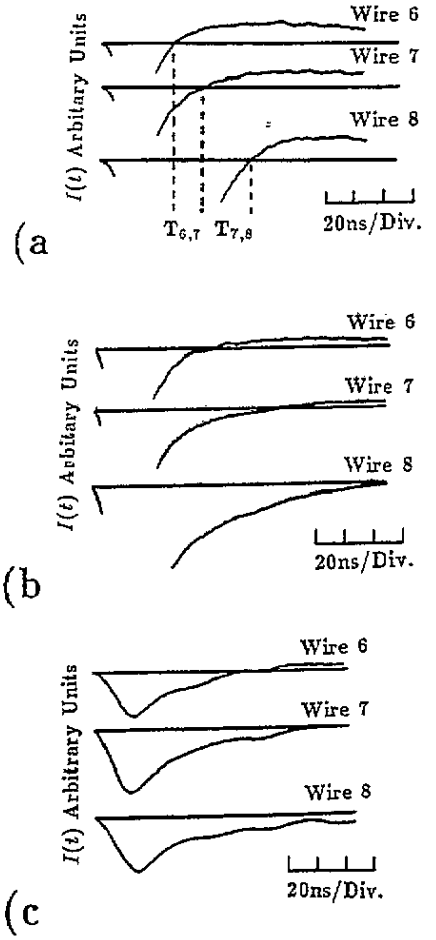

Figure 8. Field dependence of currents on wires 6, 7, and 8 induced by electrons at: (a) 4.2×10^{6} V m^{-1}, (b) 3.0×10^{6}V m^{-1} and (c) 2.0×10^{6} V m^{-1}.

not only do the profiles become more asymmetric, suggesting increased dispersive carrier propagation, but also their corresponding crossover points occur at longer times indicating, as expected, a slowing down of observed electron velocity. In fact, at low enough fields these crossover points are hardly visible. That is not to say, however, that the electrons are not drifting towards and under the wires since, if they were not, no current would be induced, but if the carrier sheet propagates under the non-Gaussian conditions shown in figure 9, as opposed to the implied Gaussian conditions in the simple model of the last section (implied because under Gaussian conditions there is actually a small spread of carrier propagation due to diffusion), then we see that its centre of charge drifts much more slowly than the faster carriers comprising it. The result would be observed currents since the electrons are drifting, but ill-defined crossovers because of a slowly moving centre of charge. From this, we therefore conclude that carrier propagation is dispersive with both its degree, and the observed electron velocity, field dependent.

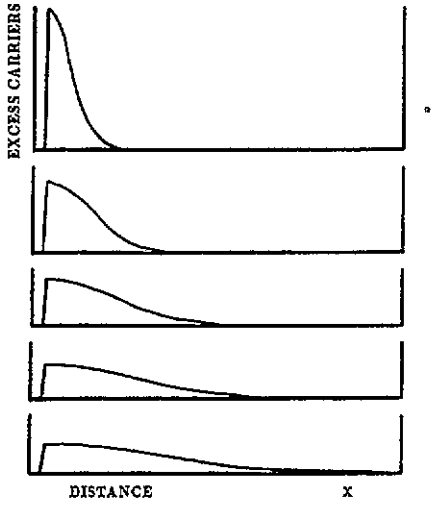

Figure 9. The carrier sheet propagating under non-Gaussian conditions.

Furthermore, this dispersion probably accounts for the time differences between adjacent crossovers increasing, and also for the current profiles becoming more asymmetric as we move further out from the initial point of carrier generation: the further out the carrier sheet drifts, the more susceptible it is to dispersion and thus the more slowly will its centre of charge drift. In view of this, it is probably not surprising that we had difficulty in obtaining clearly defined time-of-flight signals on these oxygen-rich samples using the more conventional time-of-flight techniques mentioned in section 1.

We finally consider the magnitudes of the induced currents on adjacent wires. Taking the electron case (although we could equally well consider the hole case), inspection of figure 6(a) shows that the initial photo-peak on wire 6 is appreciably smaller than those on wires 7 and 8. This is something one might not expect based on the simple model of the last section. One possibility for explaining this, however, is to consider the carrier generation event: figure 5(a) indicates that the gradient of

the induced charge ($dQ(t)/dt$) due to this initially generated carrier sheet and its subsequent drift at early times will be greater on a wire that is at a larger distance from the region of carrier creation than for a wire that is very near to it. In other words, we suggest that the initial induced current peak is greater on wires 7 and 8 than that on wire 6 by virtue of their larger displacements from the slit. In addition to this, we must also take into account the fact that some charge will drift under and away from wire 6 during the duration of the laser pulse. This would then lead to a cancelling out effect of the induced current, since charge drifting away from a wire gives rise to a current of opposite sign to charge drifting towards the it. We finally note that, as expected, the magnitudes of the photo-peaks reduce after wire 8.

Having attempted to interpret the current signals (at least qualitatively) we can now estimate the electron drift velocities and hence their mobilities. We consider figure 8(a), since those currents obtained at the highest fields exhibited the most well defined crossovers. $d/T_{6,7}$ gives a velocity of about 2500 m s^{-1} and $d/T_{7,8}$ gives a velocity of about 1400 m s^{-1}. A reasonable estimate would be their average over 100 μm and is about 1800 m s^{-1} which, at an applied field of 4.2×10^6 V m^{-1}, implies an observed mobility of 4×10^{-4} m^2 s^{-1} V^{-1}

4. Conclusions

Using this technique, time-of-flight signals for the centre of charge of a photo-generated negatively charged carrier sheet were found on what appears to be a particularly disordered material. These signals indicated that the electron velocities are acoustic, trap-limited and field dependent with observed trap-limited mobilities of the order of 10^{-4} m^2 s^{-1} V^{-1}. In addition, the fact that there was evidence of considerable dispersion of the carrier sheet at low fields (even on wire 6) implies that we are dealing with inter-trap separations on the micron level. Finally, this technique demonstrated the asymmetry that exists between electron and hole drift, with the electrons the dominant current carriers.

All these conclusions are in agreement with the transit current experiments although using this technique we are better able to estimate an upper bound for the inter-trap distances, observe clearer time-of-flight signals and also, albeit qualitatively, see the time evolution of the carrier sheet with field and with distance traversed.

There is obviously much scope for more theoretical and experimental investigation. For instance, we have assumed here that the holes drifting in one direction do not interact significantly with the signals on wires induced mainly by electrons drifting in the opposite direction. In the case of PDATS, with the holes having an apparently small mobility, this is probably justified. On other materials with a comparable hole and electron mobility this may not be the case. However, on less disordered materials (where the carrier sheet's centre of charge drifts at a velocity comparable to that of the majority of the carriers comprising it), clearer crossovers (due to the electrons say) should be visible on many wires well away from any influence due to the holes. Furthermore, the interpretations we used of the induced signals were, in effect, based on carrier position only because it was assumed initially that all the carriers drift at the same constant velocity. It is obvious that this is not the case in the material used here (though the answers obtained are not unreasonable). Once again, a less disordered material should give signals that are much clearer to interpret quantitatively.

To conclude, in principle this technique could be reduced to micron dimensions and when coupled with faster light pulses, could potentially allow access to the quantitave observation of carrier propagation (and its time evolution) on a much smaller time-scale, even on disordered materials. In addition, there is not the need to evaporate electrodes of such small gap sizes, as required in other time-of-flight experiments, which might as a result, lead to damage to the sample surface between them.

Acknowledgments

I thank Professor G Parish (University College London) and Dr D Lawunmi (Cavendish Laboratory Cambridge) for their many useful comments. I am also grateful to Professor E G Wilson (Queen Mary and Westfield College London) for suggesting this project. The experiments presented here were conducted at QMWC. This work has been supported by the SERC (UK).

References

[1] Wegner G 1969 Z *Naturf.* b **24** 824
[2] Pope M and Swenberg C E 1982 *Electronic Processes in Organic Crystals (Monographs on Physics and Chemistry of Materials 39)* (Oxford: Oxford Science Publications)
[3] Siddiqui A S and Wilson E G 1979 *J. Phys. C: Solid State Phys.* **12** 4237
[4] Donovan K J and Wilson E G 1981 *Phil. Mag.* B **44** 9
[5] Donovan K J, Elkins J W P and Wilson E G 1991 *J. Phys. C: Solid State Phys.* **3** 2075
[6] Leyrer R J, Wegner G and Wettling W 1978 *J. Phys. Chem.* **82** 697
[7] Donovan K J and Wilson E G 1985 *J. Phys. C: Solid State Phys.* **18** L51
[8] Moses D, Sinclair M and Heeger A J 1987 *Phys. Rev. Lett.* **58** 2710
[9] Moses D and Heeger A J 1989 *J. Phys.: Condens. Matter* **1** 7395
[10] Blum T and Bassler H 1988 *J. Chem. Phys.* **123** 431
[11] Fisher N E and Willock D J 1992 *J. Phys.: Condens. Matter* **4** 2517
[12] Kepler R G 1960 *Phys. Rev.* **119** 1226
[13] LeBlanc O H 1960 *J. Chem. Phys.* **33** 626
[14] Fisher N E and Willock D J 1992 *J. Phys.: Condens. Matter* **4** 2533
[15] Pfister G and Scher H 1978 *Adv. Phys.* **27** 747
[16] Scher H and Montroll E W 1975 *Phys. Rev.* B **12** 2455
[17] Siddiqui A S 1980 *J. Phys. C: Solid State Phys.* **13** L1079
[18] Yang Y, Lee J Y, Miller P, Li L, Kumar J and Tripathy S K 1991 *Solid State Commun.* **77** 763
[19] Many A and Rakavy G 1962 *Phys. Rev.* **126** 1980
[20] Many A, Weisz S Z and Simhony M 1962 *Phys. Rev.* **126** 1989
[21] Schwartz S and Hornig J E 1965 *J. Phys. Chem. Solids* **26** 1821